Hydrogen-Bonding Interaction of the Protonated Schiff Base with Halides in a Chloride-Pumping Bacteriorhodopsin Mutant†

Mikihiro Shibata,‡ Kunio Ihara,§ and Hideki Kandori*,‡

Department of Materials Science and Engineering, Nagoya Institute of Technology, Showa-ku, Nagoya 466-8555, Japan, and Graduate School of Science, Nagoya University, Chikusa-ku, Nagoya 454-8602, Japan

Received March 21, 2006; Revised Manuscript Received May 31, 2006

ABSTRACT: Bacteriorhodopsin (BR) and halorhodopsin (HR) are light-driven proton and chloride ion pumps, respectively, in *Halobacterium salinarum*. The amino acid identity of these proteins is about 25%, suggesting that each has been optimized for their own functions during evolution. However, it is known that the BR mutants, D85T and D85S, can pump chloride ions. This fact implies that the Schiff base region is important in determining ionic selectivity. The X-ray crystallographic structure of D85S(Br^-) showed the presence of a bromide ion in the Schiff base region (Facciotti, M. T., Cheung, V. S., Nguyen, D., Rouhani, S., and Glaeser, R. M. (2003) *Biophys. J. 85*, 451−458). In this article, we report on the study of hydrogen bonds of the Schiff base and water molecules in D85S in the absence and presence of various halides, assigning their N−D and O−D stretching vibrations in D_2O, respectively, in low-temperature Fourier-transform infrared (FTIR) spectroscopy. We found that the hydrogen bond of the Schiff base in D85S(Cl^-) is much stronger than that in HR, being as strong as that in wild-type BR. Similar halide dependence in D85S and in solution implies that the Schiff base forms a direct hydrogen bond with a halide, consistent with the X-ray structure. Photoisomerization causes a weakened hydrogen bond of the Schiff base, and halide dependence on the stretching frequency is lost. These spectral features are similar to those in the photocycle of proton-pumping BR, though the weakened hydrogen bond is more significant for BR. However, the spectral features of water bands in D85S are closer to chloride-pumping HR because O−D stretching vibrations of water are observed only at >2500 cm^{-1}. Unlike in BR, we did not observe strongly hydrogen-bonded water molecules for halide-pumping D85S mutants. This observation agrees with our recent hypothesis that strongly hydrogen-bonded water molecules are required for the proton-pumping activity of archaeal rhodopsins. Hydrogen-bonding conditions in the Schiff base region of D85S are discussed on the basis of the spectral comparison with those of wild-type BR and HR.

Photosynthesis in some archaea involves two rhodopsins that do not utilize electron-transfer reactions. Bacteriorhodopsin (BR)[1] and halorhodopsin (HR) in *Halobacterium salinarum* function as light-driven proton and chloride pumps, respectively (*1*-*4*). The chromophore of these proteins is all-trans retinal that binds to a lysine residue through a Schiff base linkage, and the all-trans to 13-cis photoisomerization triggers the pumping process. Extensive studies on BR have suggested the mechanism for unidirectional translocation of protons (*1*, *2*). In contrast, the molecular mechanism of chloride transport in *Halobacterium salinarum* HR (*s*HR) and a homologous HR from *Natronomonas pharaonis* (*p*HR) is still poorly understood.

In 1995, Sasaki et al. reported that the replacement of the amino acid at position 85 from Asp to Thr converts BR from a proton to chloride pump (*5*). Later, it was found that the D85S mutant more strongly binds chloride and also pumps chloride ions (*6*). D85T and D85S also pump other halide ions as well as HR. In the absence of halide, the absorption maximum of D85S is located at about 600 nm (*7*). Halide binding to D85S shifts the absorption maximum at about 570 nm, apparently because the halide becomes the counterion of the protonated Schiff base.

Figure 1 shows the Schiff base region of BR (*8*), D85S mutant in the absence (*9*, *10*) and presence of Br^- (*11*), and *s*HR (*12*). The structure of the Schiff base region is similar in BR and *s*HR. It contains a quadrupole with positive charges located at the protonated Schiff base and Arg82 (Arg108 in *s*HR) and counterbalancing negative charges located at Asp85 (chloride ion in *s*HR) and Asp212 (Asp238 in *s*HR). Such structural similarity could lead to the functional interconversion from a proton to chloride ion pump in BR. However, the Schiff base region of D85S is considerably different from that of BR and *s*HR (Figure 1). The hydrogen-bonding acceptor of the Schiff base is a water molecule in BR and *s*HR, whereas the N−H group of the

† This work was supported by grants from the Japanese Ministry of Education, Culture, Sports, Science, and Technology to H.K. (15076202) and Research Fellowships from the Japan Society for the Promotion of Science for Young Scientists to M.S.

* To whom correspondence should be addressed. Phone: 81-52-735-5207. Fax: 81-52-735-5207. E-mail: kandori@nitech.ac.jp.

‡ Nagoya Institute of Technology.

§ Nagoya University.

[1] Abbreviations: BR, bacteriorhodopsin; *s*HR, *salinarum* halorhodopsin; *p*HR, *pharaonis* halorhodopsin; FTIR, Fourier-transform infrared; 5-FOA, 5-fluoroorotate.

10.1021/bi060555s CCC: $33.50
Published on Web 08/10/2006

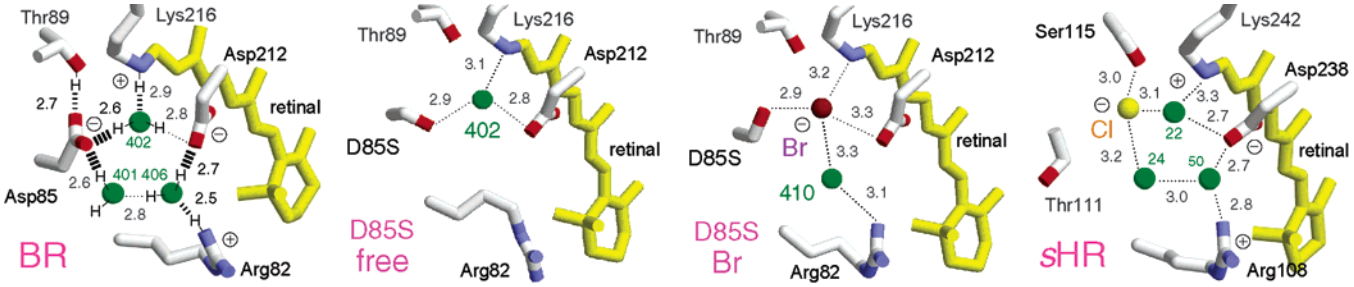

FIGURE 1: X-ray crystallographic structures of BR (pdb entry 1C3W (*8*)), halide-free D85S mutant of BR (pdb entry 1S8L (*10*)), Br^--bound D85S mutant of BR (pdb entry 1MGY (*11*)), and *s*HR (pdb entry 1E12 (*12*)). The membrane normal is approximately in the vertical direction of this Figure. Upper and lower regions correspond to the cytoplasmic (CP) and extracellular (EC) sides, respectively. Green spheres represent water molecules bound inside each protein. Hydrogen atoms of the Schiff base, Thr89, Arg82, and water molecules in BR are from refs *21*, *46*, *47*, and *25*, respectively. In other panels, hydrogen bonds (·····) are supposed from the structure, and the numbers are the hydrogen-bonding distances in Å.

Schiff base in D85S(Br^-) seems to form a hydrogen bond directly with the bromide ion. D85S contains only one water molecule in the Schiff base region regardless of the absence or presence of bromide. Thus, an analysis of hydrogen bonds in D85S is important to understand the mechanism of light-driven ion pumps.

Hydrogen-bonding strength of the protonated Schiff base in rhodopsins has been studied from the C=N stretching vibrations in resonance Raman or FTIR spectroscopy. The difference in frequency between the C=NH and C=ND stretching vibrations is regarded as the marker of hydrogen-bonding strength because a stronger hydrogen bond yields a larger difference (*13*, *14*). On the basis of this, resonance Raman and FTIR spectroscopy reported the hydrogen-bonding strength in *s*HR (*15*, *16*), *p*HR (*17*), and the L-intermediate of *s*HR (*18*). However, halide dependence on the hydrogen-bonding strength of the Schiff base has not been clearly understood. One reason could be that the C=N stretch is a skeletal vibration of the retinal chromophore, and the observed C=N stretching vibrations did not change significantly among different halides. Consequently, the difference between C=NH and C=ND stretching frequencies was also tiny, leading to the difficulty in determining halide dependence. In contrast, the N−H stretching mode is a more direct probe of the hydrogen-bonding strength of the Schiff base. In fact, Lussier et al. reported the N−H stretching frequencies of the all-trans retinal protonated Schiff base in $CDCl_3$ at 2600, 2735, and 2957 cm^{-1} in the presence of Cl^-, Br^-, and I^-, respectively (*19*). In solution, the halide ion is located at the most stable position relative to the Schiff base, where the Schiff base N−H group presumably forms a direct hydrogen bond with the halide ion. Thus, we can state that if the Schiff base forms a hydrogen bond with halide directly, the N−H stretching mode of the Schiff base will be upshifted when the halide ion is larger, even in a protein environment. However, as is easily imagined, the strong absorption of water molecules masks such an N−H stretching vibration of the Schiff base.

In 1998, we reported accurate K minus BR difference spectra at 77 K for the entire X−H (X−D in D_2O) stretching region (4000−1800 cm^{-1}) (*20*). This constituted progress because it allowed the direct detection of the stretching modes of the Schiff base and water, whose signals could now be well analyzed in D_2O. With the use of a [ζ-^{15}N]-Lys-labeled sample, we identified the N−D stretches of the Schiff base in BR at 2173 and 2123 cm^{-1}, which shifts to 2495 and 2468 cm^{-1} in the K intermediate (*21*). Recently, we extended the analysis to *p*HR, and successfully assigned the N−D stretching vibrations of the Schiff base for various halide ions (*22*). Interestingly, halide dependence revealed that the Schiff base forms a direct hydrogen bond with halide only in the K intermediate, and not in *p*HR or the L-intermediate. This finding resulted in a revision of the model of the primary process in chloride transport because direct Schiff base and halide interaction had been postulated before for both unphotolyzed and intermediate states (*4*, *7*, *12*). The hydrogen bond of the Schiff base is further strengthened in the L_1-intermediate, whereas halide dependence revealed that the acceptor is not Cl^- but presumably a water molecule (*22*).

Analysis of water molecules is another highlight of our FTIR study. We reported O−D stretching vibrations of internal water molecules in BR (*23*−*25*) and *p*HR (*22*). BR contains water molecules with O−D stretching vibrations at <2400 cm^{-1}, indicating that these waters form very strong hydrogen bonds (Figure 1) (*23*). By using several BR mutants, we suggested that such water molecules are in the Schiff base region (*24*, *25*). Similar FTIR studies of the later intermediates of BR led to the proposal of the hydration switch model, which explains the proton transfer from the Schiff base to Asp85 (*26*) with an internal water molecule that directs the proton transfer by changing its hydrogen bond from Asp85 to Asp212. FTIR studies of BR mutants and other rhodopsins have provided an empirical rule between strongly hydrogen-bonded water molecules and proton-pumping activity (*27*). Our hypothesis is that strongly hydrogen-bonded water molecules are required for the proton-pumping activity of archaeal rhodopsins. However, strongly hydrogen-bonded water molecules are absent in HR (*28*). Here, an internal water molecule seems to act as the hydrogen-bond acceptor of the Schiff base in the L_1-intermediate during chloride transport. Then, how is the hydrogen bond of the internal water molecule in D85S? How does halide-binding change the hydrogen-bonding structure of D85S?

In this article, we report on the hydrogen-bonding interaction of the Schiff base and internal water molecules in D85S by means of low-temperature FTIR spectroscopy. We trapped the K intermediate at 130 K, and difference FTIR spectra were recorded in the absence and presence of Cl^-, Br^-, and I^-. The C=N and the N−D stretches of the Schiff base were assigned by use of [ζ-^{15}N]Lys-labeled D85S, whereas O−D

stretches of water were assigned by comparing spectra in D_2O and $D_2{}^{18}O$. Although the difference in the frequency between C=NH and C=ND stretching vibrations did not show halide dependence, clear halide dependence was observed for the N−D stretching vibration of the Schiff base in D85S as well as in solution. We conclude that the Schiff base forms a direct hydrogen bond with halide in the unphotolyzed state of D85S, as in the X-ray crystal structure (*11*). Strongly hydrogen-bonded water molecules are not present in D85S regardless of the absence or presence of halides. Hydrogen-bonding conditions in the Schiff base region of D85S are discussed on the basis of the present FTIR spectral analysis.

MATERIALS AND METHODS

Plasmid Constructs and Site-Directed Mutagenesis. A fragment containing the bop gene (1.6 kbp) was amplified by PCR and cloned into the vector pGEM-T easy (Promega) using the primer set (5′-ggatccGACGTGAAGATGGGGC-3′, 5′-ggatccGTGACCGTTCGATGC-3′). A cloned fragment was confirmed for its sequence and then transferred to the vector pUC18 for mutagenesis or the vector pMPK54 for transformation (*29*), which contains a gene conferring resistance to the 3-hydroxy-3-methylglutaryl CoA reductase inhibitor simvastatin in *H. salinarum*. A point mutation (Asp85 → Ser) was introduced into the bop gene by PCR mutagenesis (Stratagene), and resultant mutation was confirmed by sequencing the plasmids prior to the transformation of *H. salinarum*.

Transformation for H. salinarum and Cultivation for Isotope Labeling. *H. salinarum* strains MPK409 (*29*) were transformed using the plasmid described above. The transformation procedure was essentially the same as that described in a previous article (*30*). Briefly, 10 mL of early log phase cells were collected by centrifugation (6000 *g*, 10 min) and resuspended in 2 mL of spheroplasting solution. Then, 100 mL aliquots were added to 10 mL of 0.5 M EDTA in spheroplasting solution and gently mixed. After 20 min, 3−5 mg of plasmid DNA in 10 mL was added and incubated for a further 10 min. Equal volumes (140 mL in this case) of 60% poly(ethylene glycol) 600 in spheroplasting solution was added and mixed by gently tilting the tube back and forth. After 20 min of additional incubation, 1 mL of regeneration salt solution was added. The cells were pelleted in a microcentrifuge at 5000 rpm for 5 min, and to the resultant pellet, 1 mL of complex culture medium containing 15% sucrose was added. After incubation for 48 h at 37 °C, 100 μL samples were spread on plates containing 15% sucrose and 10 μg/mL simvastatin. After 10 days of incubation at 40 °C, purple colored colonies were picked and grown in complex cuture medium with 10 mg/mL of simvastatin, and after incubation for 24 h at 37 °C, 100 mL samples were spread on plates containing 250 μg/mL of 5-FOA. After a week of incubation, purple colonies were picked and grown again in complex cuture medium containing 50 μg/mL of uracil. For preparing [ζ-^{15}N]L-Lys-labeled sample, [ζ-^{15}N]L-Lys (0.1 g/L)was replaced by unlabeled L-Lys in the amino acid synthetic growth medium (*31*) containing 50 μg/mL of uracil. The purple membranes were isolated and purified in the usual manner (*32*).

Sample Preparation for FTIR Measurements. Samples were prepared in 2 mM citrate buffer (pH 5.0) in the presence of 1.6 mM Na_2SO_4, 5 mM NaCl, NaBr, and NaI and centrifuged three times to replace each halide (*22*). A 120 μL aliquot of the sample was dried on a BaF_2 window with a diameter of 18 mm. After hydration by 1 μL of H_2O, D_2O, or $D_2{}^{18}O$, the sample was placed in a cell and then mounted on an Oxford DN-1704 cryostat. Absorption maxima of the hydrated films were at 596 nm in the absence of halide and at 565, 566, and 561 nm in the presence of Cl^-, Br^-, and I^-, respectively. The hydrated film was illuminated with >500 nm light for 2 min at 230 K to obtain the light-adapted state of D85S.

Low-temperature FTIR spectroscopy was applied as described previously by using a Bio-Rad FTS-40 FTIR spectrometer (*20*−*26*). Because the orientation of molecules in hydrated films was not good, we did not use an IR polarizer in the FTIR measurements, and the sample films were not tilted in the cryostat. The K minus D85S spectra were measured by photoconversion between the K and unphotolyzed states at 130 K (*20*, *21*, *23*−*25*). Spectral resolution was 2 cm^{-1}, and 40 spectra of 128 interferograms were averaged. The spectral features were similar to those of the wild type in the 1800−800 cm^{-1} region, indicating the formation of the K intermediate. Each spectrum was normalized at the 1202 cm^{-1} (−) band because of the C−C stretch of the retinal chromophore. The spectra of D85S-(free) are shown without changing the amplitude, whereas those for D85S(Cl^-) and D85S(Br^-) were multiplied by a factor of 0.7, and those for D85S(I^-) were multiplied by a factor of 1.2.

RESULTS

Assignment of the C=N Stretching Vibration of the Protonated Schiff Base in D85S and Its K Intermediate. In this study, we prepared the [ζ-^{15}N]Lys-labeled D85S samples to assign vibrational modes of the protonated Schiff base. It is noted that ^{15}N-labeling did not cause any substantial changes in other bands. Figure 2 shows the spectral changes in the frequency region of the C=N stretching mode of the retinal Schiff base in H_2O, where the isotope-sensitive bands can be assigned as C=NH stretching vibrations of the Schiff base. In the wild type of BR, the C=N stretching vibrations were reported to be 1641 and 1608 cm^{-1} for the unphotolyzed and K states, respectively, by means of FTIR spectroscopy (*33*). In D85S, the intensities of the broad negative bands at 1632 (free), 1632 (Cl^-), 1631 (Br^-), and 1629 (I^-) cm^{-1} are significantly reduced in the [ζ-^{15}N]Lys-labeled D85S sample (Figure 2A). From the double difference spectra, which subtracts the labeled spectra from unlabeled ones (Figure 2B), we assigned the C=NH stretch in the unphotolyzed state of D85S as shown in Table 1. Earlier FTIR spectroscopy of sHR also reported that the C=NH stretching vibrations of the Schiff base differ among halides (*18*).

Upon formation of the K intermediate, positive peaks appear in the 1620−1600 cm^{-1} region (Figure 2A). The two peaks that exhibit isotope shift from the [ζ-^{15}N]Lys-label, the bands at 1622 and 1612 cm^{-1}, are candidates for the C=NH stretch of the K intermediate of D85S(Cl^-). It should be noted that the C=O stretch of the peptide carbonyl (amide I vibration) of Val49 appears at 1623 (+)/1617 (−) cm^{-1} for wild-type BR (*34*). Spectral shapes of D85S at around

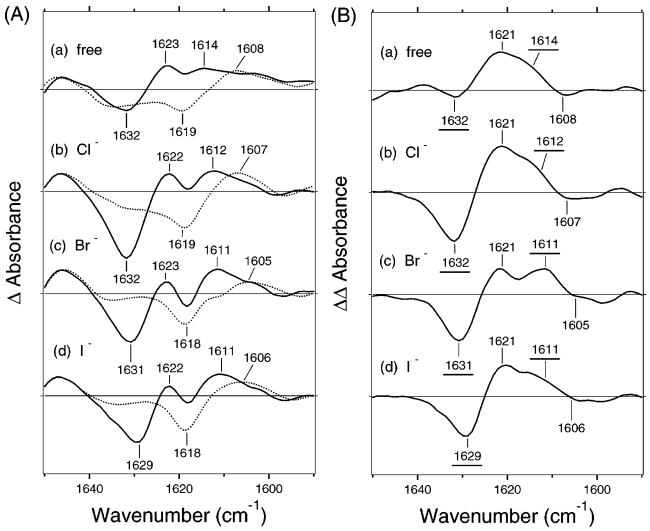

FIGURE 2: (A) K minus D85S difference infrared spectra of halide-free (a), Cl^--bound (b), Br^--bound (c), and I^--bound (d) D85S in the 1770−1560 cm^{-1} region. Unlabeled (—) and [ζ-^{15}N]Lys-labeled (····) D85S samples were hydrated with H_2O, and spectra were measured at 130 K. One division of the *y* axis corresponds to 0.002 absorbance units. (B) Double difference spectra of [ζ-^{15}N]Lys-labeled and unlabeled samples, where the spectra of the labeled D85S are subtracted from those of the unlabeled D85S in panel A. Underlined frequencies of the negative and positive bands correspond to the C═NH stretching vibrations in the unphotolyzed and K states, respectively.

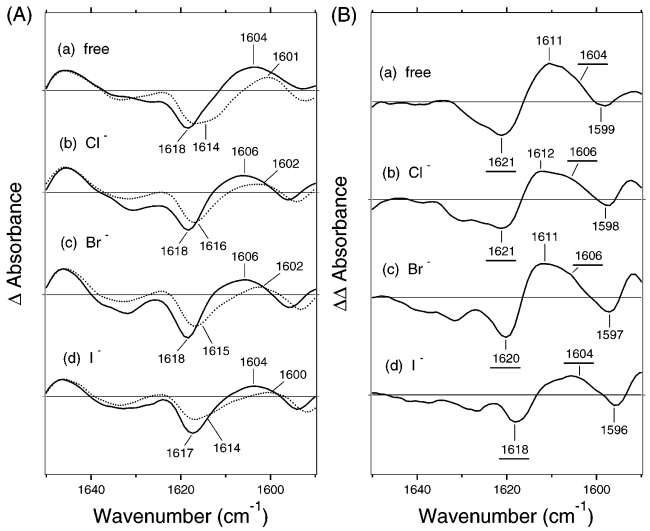

FIGURE 3: (A) K minus D85S difference infrared spectra of halide-free (a), Cl^--bound (b), Br^--bound (c), and I^--bound (d) D85S in the 1770−1560 cm^{-1} region. Unlabeled (—) and [ζ-^{15}N]Lys-labeled (····) D85S samples were hydrated with D_2O, and spectra were measured at 130 K. One division of the *y* axis corresponds to 0.002 absorbance units. (B) Double difference spectra of [ζ-^{15}N]Lys-labeled and unlabeled samples, where the spectra of the labeled D85S are subtracted from those of the unlabeled D85S in panel A. Underlined frequencies of the negative and positive bands correspond to the C═ND stretching vibrations in the unphotolyzed and K states, respectively.

Table 1: Frequencies of the C═N and N−D Stretching Vibrations of the Schiff Base in the Wild-Type and D85S Bacteriorhodopsin

		C═NH stretch (cm^{-1})	C═ND stretch (cm^{-1})	$\Delta\nu_{H/D}$ (cm^{-1})	N−D stretch (cm^{-1})
wild type	BR	1641[a]	1628[a]	13	2173[b], 2123[b]
	K	1608[a]	1606[a]	2	2466[b], 2495[b]
D85S (free)	BR	1632	1621	11	2280, 2224
	K	1614	1604	10	2306
D85S (Cl^-)	BR	1632	1621	11	2166, 2209, 2109
	K	1612	1606	6	2312
D85S (Br^-)	BR	1631	1620	11	2241, 2209, 2109
	K	1611	1606	5	2312
D85S (I^-)	BR	1629	1618	11	2255, 2209, 2109
	K	1611	1604	7	2312

[a] From ref *32*. [b] From ref *21*.

1620 cm^{-1} (Figure 2A) are similar to that of the wild type, suggesting that the same amide-I bands of Val49 are involved in the spectra of D85S. Therefore, we examined the double difference spectrum, where the contribution of amide-I bands is canceled. Figure 2B shows two positive peaks, between which a higher frequency band (1621 cm^{-1}) originates from the C═^{15}NH stretch of the unphotolyzed state as judged from the original spectra (dotted lines in Figure 2A). Thus, we assigned the C═NH stretches of the K intermediate in D85S at 1614 (free), 1612 (Cl^-), 1611 (Br^-), and 1611 (I^-) cm^{-1} (Table 1).

Figure 3 shows the spectral changes in the frequency region of the C═ND stretching mode of the retinal Schiff base in D_2O, where the isotope-sensitive bands can be assigned as C═ND stretching vibrations of the Schiff base. In wild type BR, the C═ND stretching vibrations were reported to be 1628 and 1606 cm^{-1} for the unphotolyzed and K states, respectively, by means of FTIR spectroscopy (*33*). As described above, the amide-I bands of Val49 appear at 1623 (+)/1617 (−) cm^{-1}, which do not shift in D_2O. For this reason, the negative peaks at 1617 to 1618 cm^{-1} may not represent the C═ND stretch of the Schiff base accurately. Figure 3B shows double difference spectra between unlabeled and [ζ-^{15}N]Lys-labeled D85S. From the negative peak at around 1620 cm^{-1}, we assigned the C═ND stretch in the unphotolyzed state of D85S at 1621 (free), 1621 (Cl^-), 1620 (Br^-), and 1618 (I^-) cm^{-1} (Table 1).

Upon the formation of the K intermediate, positive peaks appear in the 1610−1590 cm^{-1} region, which exhibit spectral downshift by [ζ-^{15}N]Lys-labeling (Figure 3A). Therefore, we assigned the C═ND stretch in the K intermediate of D85S at 1604 (free), 1606 (Cl^-), 1606 (Br^-), and 1604 (I^-) cm^{-1} (Table 1). The double difference spectra in Figure 3B also support the assignment.

From ^{15}N-isotope labeling of the side chain of lysine, we assigned the C═NH and C═ND stretches of the Schiff base in the unphotolyzed and K states of D85S. Figure 4 shows infrared difference spectra of D85S hydrated with H_2O (solid lines) and D_2O (dotted lines), where the tagged frequencies in the 1650−1600 cm^{-1} region originate from C═NH and C═ND stretches of the Schiff base, respectively. Interestingly, the frequency difference between C═NH and C═ND stretching vibrations in the unphotolyzed state (11 cm^{-1}) is not halide dependent, which has been regarded as the marker of the hydrogen-bonding strength of the Schiff base (Table 1). According to the X-ray crystal structure (Figure 1), the N−H group of the Schiff base forms a direct hydrogen bond with Br^-. This suggests that other halides such as Cl^- and I^- occupy the same position as that of Br^-. If this is the case, could the hydrogen-bonding strength of the Schiff base be identical among different halides? In addition, the value

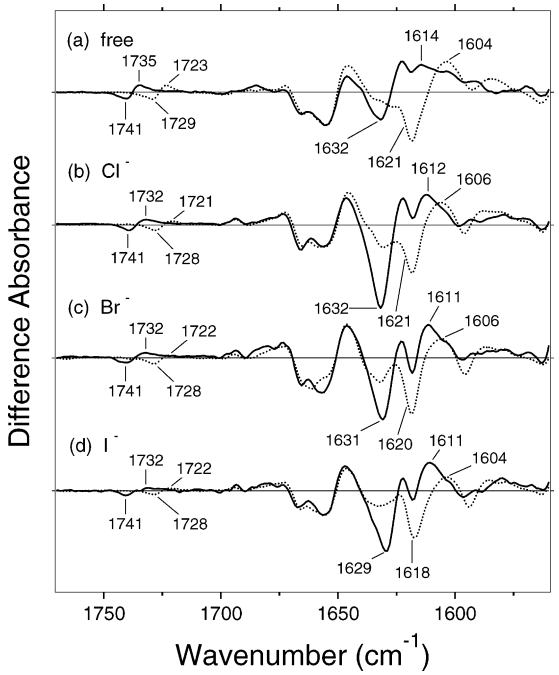

FIGURE 4: K minus D85S difference infrared spectra of halide-free (a), Cl^--bound (b), Br^--bound (c), and I^--bound (d) D85S in the 1770−1560 cm^{-1} region. The samples were hydrated with H_2O (—) or D_2O (····), and spectra were measured at 130 K. One division of the *y* axis corresponds to 0.002 absorbance units.

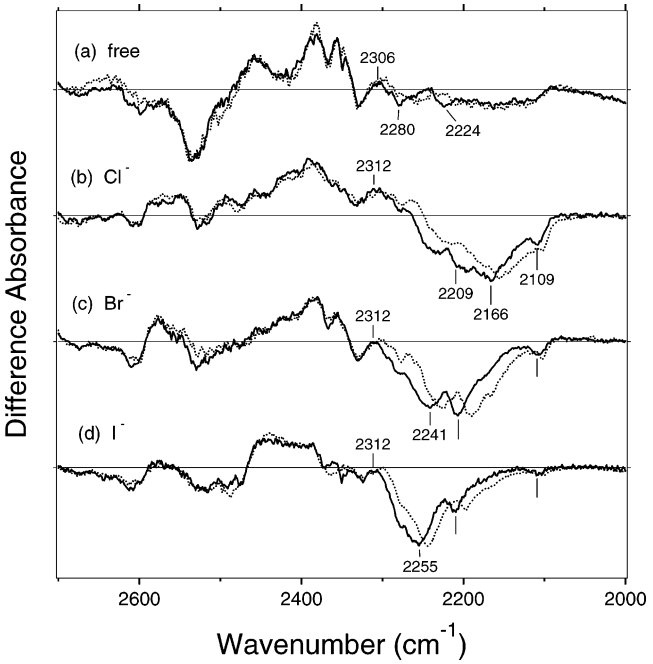

FIGURE 5: K minus D85S difference infrared spectra of halide-free (a), Cl^--bound (b), Br^--bound (c), and I^--bound (d) D85S in the 2700−2000 cm^{-1} region. Unlabeled (—) and [ζ-^{15}N]Lys-labeled (····) D85S samples were hydrated with D_2O, and spectra were measured at 130 K. One division of the *y* axis corresponds to 0.00018 absorbance units.

(11 cm^{-1}) is also identical to that measured in halide-free D85S. According to the X-ray crystal structure of the free form (Figure 1), a water molecule is a hydrogen-bonding acceptor of the Schiff base. Although D85S(free) lacks a negative charge in the Schiff base region, is the hydrogen-bonding strength of the Schiff base with water identical to that with halides? As we showed previously (*21*), the N−D stretching vibration in D_2O is a more direct probe of hydrogen-bonding strength, and more detailed information will be gained. We analyze the N−D stretches in the following section.

Figure 4 provides different information about D85S. The 1750−1700 cm^{-1} region is characteristic of frequencies of the C═O stretch of protonated carboxylic acids. Figure 4 shows the bands at 1741 (−)/1735 (+) cm^{-1} for the halide-free form and at 1741 (−)/1732 (+) cm^{-1} for the halide-bound forms. Spectral downshifts by 11−13 cm^{-1} were observed upon D_2O hydration. The bands probably originate from Asp115, as is the case for the wild-type and mutant BR (*35*). However, no additional bands were observed in Figure 4. In a previous study of the NO_3^--bound D85S, it was suggested that Asp212 is protonated (*10*). Protonation of Asp212 is also reasonable for halide-bound D85S because the distance between Asp212 and halide is short (3.3 Å for Br^-, Figure 1). However, the K minus D85S spectra do not show additional bands for any halide-bound forms.

Assignment of the N−D Stretching Vibration of the Protonated Schiff Base in D85S and Its K Intermediate in D_2O. Figure 5 compares K minus D85S spectra between unlabeled (solid lines) and [ζ-^{15}N]Lys-labeled (dotted lines) samples in the X−D stretching frequency region. In the halide-free D85S, two negative bands at 2280 and 2224 cm^{-1} exhibit isotope shifts, indicating that they originate from N−D stretching vibrations of the Schiff base in the unphotolyzed state (Figure 5a). Although the isotope shift was small for D85S(free), a prominent isotope shift was observed for the negative bands of halide-bound D85S. Indeed, a broad negative feature at 2300−2100 cm^{-1} entirely exhibits isotope shifts of [ζ-^{15}N]Lys-labeling, indicating that they originate from N−D stretching vibrations of the Schiff base in the unphotolyzed state (Figure 5b−d). Despite such a common spectral feature, interestingly, clear halide dependence was observed. In D85S(Cl^-), the largest negative peak appears at 2166 cm^{-1} (Figure 5b). Peaks are also observed at 2209 and 2109 cm^{-1}. However, two strong negative peaks appeared at 2241 and 2209 cm^{-1} for D85S(Br^-) (Figure 5c), whereas an intense negative peak appeared at 2255 cm^{-1} for D85S(I^-) (Figure 5d). The centers of gravity for the negative bands were calculated to be 2178, 2218, and 2239 cm^{-1} for Cl^--, Br^--, and I^--bound forms, respectively. Thus, it is revealed that the frequency is lowered as halide becomes smaller. Such halide dependence was not clearly observed in the analysis of the C═N stretch.

It should be noted that the N−H stretching frequencies of the all-trans retinal Schiff base in $CDCl_3$ are located at 2600, 2735, and 2957 cm^{-1} in the presence of Cl^-, Br^-, and I^-, respectively (*19*). Corresponding N−D stretching frequencies are located at 2150−1900 cm^{-1}. Halide dependence on the N−D stretching vibration of the Schiff base in D85S was found to be similar to that in solution. In solution, the N−H (N−D) group of the Schiff base presumably forms a direct hydrogen bond with halides. Therefore, the present study strongly suggests that the Schiff base forms a direct hydrogen bond with a halide ion in D85S. The present FTIR results are consistent with the X-ray crystal structure (*11*).

The N−D stretching frequencies have been reported to be at 2173 and 2123 cm^{-1} for BR (*21*), at 2488 cm^{-1} for *p*HR(Cl^-) (at 2480 cm^{-1} for *p*HR(Br^-), and at 2458 cm^{-1}

for *p*HR(I^-)) (*22*), where a lower frequency corresponds to a strong hydrogen bond. In this view, the Schiff base forms a strong hydrogen bond with halides in D85S because their N−D stretching frequencies are at 2250−2150 cm^{-1}. Although the N−D stretching vibrations are halide dependent, it seems that the halide-independent peak is present. For instance, a negative band at 2109 cm^{-1} is commonly observed among three halides. A negative band at 2209 cm^{-1} also may be common. In contrast, peaks at 2166, 2241, and 2255 cm^{-1} are unique for Cl^--, Br^--, and I^--bound forms, respectively. Multiple N−D stretch bands also have been reported for BR (2173 and 2123 cm^{-1}) (*21*) and *pharaonis* phoborhodopsin (2140 and 2091 cm^{-1}) (*36*).

Unlike the negative bands, a positive N−D stretch was not clearly observed in Figure 5. One possibility is that the frequency is close to those of the negative bands. In fact, the frequency differences of C═NH and C═ND stretches for the K states of D85S are larger (5−10 cm^{-1}) than that for the K state of the wild type (2 cm^{-1}), suggesting that the hydrogen bond of the Schiff base is not more weakened for D85S. No bands were actually affected by the [ζ-^{15}N]Lys-labeled D85S sample at >2400 cm^{-1}. However, the positive band at 2306 cm^{-1} in Figure 5a exhibits isotope shift upon [ζ-^{15}N]Lys-labeling. Similarly, the positive band at 2312 cm^{-1} in Figure 5b exhibits spectral downshift upon [ζ-^{15}N]-Lys-labeling. Therefore, we assign the N−D stretch of the K states of D85S(free) and D85S(Cl^-) to the 2306 and 2312 cm^{-1} bands, respectively (Table 1). Regarding D85S(Br^-) and D85S(I^-), Figure 5c and d shows isotope-induced spectral downshifts for the positive 2312-cm^{-1} band, though they do not appear at the positive side. We infer that it is due to the strong negative bands. Thus, we assigned that the N−D stretches of the K states of D85S(Br^-) and D85S(I^-) at 2312 cm^{-1} (Table 1). On the basis of the present assignment, there is no halide dependence for the N−D stretches of the Schiff base (2312 cm^{-1}) in the K intermediate in contrast to those in the unphotolyzed state. The value is also close to that for the free-form (2306 cm^{-1}). These observations suggest that the N−D group of the Schiff base does not form a direct hydrogen bond with a halide in the K intermediate. Interestingly, a lack of halide dependence does not mean that the hydrogen bond of the Schiff base is broken because its frequency at about 2310 cm^{-1} implies a hydrogen bond for the Schiff base. This may suggest that in K, the Schiff base finds another hydrogen-bonding acceptor.

Assignment of the O−D Stretching Vibration of Water Molecules in D85S and Its K Intermediate in D_2O. Figure 6 compares the K minus D85S spectra between samples hydrated with D_2O (red spectra) and $D_2{}^{18}O$ (blue spectra) in the O−D stretching frequency region. In the halide-free D85S, ^{18}O-water-induced isotope shifts are observed for the two negative bands at 2610 and 2583 cm^{-1} and for a positive band at 2458 cm^{-1} (Figure 6a). Two negative and one positive band are also observed at 2610, 2529 cm^{-1}, and 2568 cm^{-1}, respectively, for D85S(Cl^-) and D85S(Br^-) (Figure 6b and c). In contrast, only one peak pair is observed at 2610 (−)/2568 (+) cm^{-1} for D85S(I^-) (Figure 6d). There are no water bands at <2400 cm^{-1} for halide-bound forms (Figure 6b−d). In the case of D85S(free), the 2400−2200 cm^{-1} region is noisy, but no clear isotope shift of water can be observed (Figure 6a). It should be noted that wild-type BR contains strongly hydrogen-bonded water molecules,

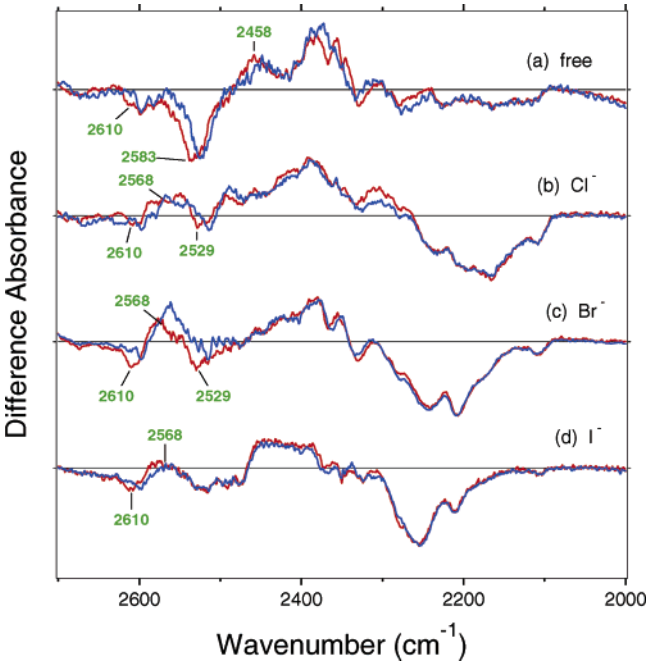

FIGURE 6: K minus D85S difference infrared spectra of the absent halide (a), containing Cl^-- (b), Br^-- (c), or I^--bound (d) forms in the 2700−2000 cm^{-1} region. The sample was hydrated with D_2O (red curves) or $D_2{}^{18}O$ (blue curves), and spectra were measured at 130 K. Green-labeled frequencies correspond to those identified as stretching vibrations of water O−D. One division of the *y* axis corresponds to 0.00018 absorbance units.

whose O−D stretches are located at 2350−2150 cm^{-1} (*23*−*25*). A recent FTIR study showed that strongly hydrogen-bonded water molecules are only found in rhodopsins with proton-pumping activity (*27*), whereas strongly hydrogen-bonded water molecules are absent in HR (*28*). The present results clearly show that the functionally converted mutant BR (D85S) from proton pump to halide pump does not possess strongly hydrogen-bonded water molecules, consistent with the empirical rule.

Two frequencies of water are separated by ~80 cm^{-1} for D85S(Cl^-) and D85S(Br^-) (Figure 6b and c). In general, a water molecule has two O−H groups, and their frequencies are distributed in the wide 3700−2700 cm^{-1} region dependent on their coupling and hydrogen-bonding strength. Gaseous water exhibits asymmetric and symmetric stretching modes at 3755 and 3657 cm^{-1}, respectively, and the stretching frequency is lowered because its hydrogen bond becomes stronger (*37*). Corresponding asymmetric and symmetric O−D stretching modes appear at about 2788 and 2671 cm^{-1}, respectively (*38*). We thereby infer that the bands at 2610 and 2529 cm^{-1} in D85S(Cl^-) and D85S(Br^-) correspond to asymmetric and symmetric stretching modes of a water molecule, respectively. Because the X-ray crystal structure of D85S(Br^-) shows the presence of a water molecule (water410) near Br^- (Figure 1), the observed water bands may originate from water410. However, the lack of halide dependence may suggest a role for another water molecule.

DISCUSSION

The present low-temperature FTIR spectroscopic study successfully assigned the vibrational frequencies of the N−D stretch of the Schiff base and O−D stretches of internal water

molecules in D85S. In the earlier studies of vibrational analysis, the hydrogen strength of the N−H group of the protonated Schiff base was evaluated from the difference in frequencies between the C=NH and C=ND of the protonated Schiff base (*14*). However, this approach does not appear to be suitable for the study of halide-binding rhodopsins. Previous vibrational analysis of the C=NH and C=ND for *s*HR or *p*HR could not provide halide dependence on the hydrogen-bonding strength of the Schiff base. In contrast, in a recent FTIR study we observed clear halide dependence by analysis of N−D stretching vibrations, and a new model of the primary process of chloride transport has been established on the basis of the results (*22*). The estimate of hydrogen-bonding strength of the Schiff base from the C=N stretch band is probably less sensitive than that by N−D stretches for various halides.

This correlation was also the case for the BR mutant in the present study. The frequency differences between the C=NH and C=ND stretches were identical among three halides (11 cm^{-1}; Table 1), suggesting identical hydrogen-bonding strengths. However, entirely different results were obtained from the N−D stretching vibrations of the Schiff base, where a clear halide dependence was observed. The N−D stretching frequencies were lowest for D85S(Cl^-) and highest for D85S(I^-), and such halide dependence was the same as the N−H stretches vibration of the all-trans retinal Schiff base in solution (*19*). This implies that in D85S, the Schiff base forms a direct hydrogen bond with halide. This result is consistent with the X-ray crystal structure of D85S in the presence of Br^- (*11*).

Upon formation of the K intermediate, the halide dependence is lost for the N−D stretch bands of the Schiff base (Figure 5). These observations suggest that the N−D group of the Schiff base does not form a direct hydrogen bond with a halide in the K intermediate. Lack of halide dependence does not mean a broken hydrogen bond of the Schiff base because the frequency at about 2310 cm^{-1} implies that the Schiff base retains a hydrogen bond. This may suggest that the Schiff base finds another hydrogen-bonding acceptor, such as Thr89, Tyr185, Asp212, or a water molecule.

Recently, we proposed a model for chloride ion pumping in *p*HR from the analysis of the N−D stretching vibration of the Schiff base and the O−D stretching vibrations of water molecules (*22*). The halide dependence of the stretching vibrations enabled us to conclude that the Schiff base forms a direct hydrogen bond with Cl^- only in the K intermediate. The hydrogen bond of the Schiff base is further strengthened in the L_1-intermediate, whereas halide dependence revealed that the acceptor is not Cl^- but presumably a water molecule. Thus, we concluded that the hydrogen-bonding interaction between the Schiff base and Cl^- is not a driving force of the motion of Cl^-. Rather, the removal of its hydrogen bonds with the Schiff base and water(s) makes the environment around Cl^- less polar in the L_1-intermediate, which presumably drives the motion of Cl^- from its binding site to the cytoplasmic domain (*22*). To study the mechanism of chloride transport in D85S, we have to study late photocycle intermediates. The present results suggest that the lack of halide dependence of the Schiff base in the intermediates where the crucial translocation of the halide occurs may be a key element for the chloride pump.

Previous FTIR studies of BR mutants and various rhodopsins have provided an empirical rule between strongly hydrogen-bonded water molecules and proton-pumping activity (*27*). In the study, we found that BR (*23*), *pharaonis* phoborhodopsin (*39*), *Leptosphaeria* rhodopsin (*40*), proteorhodopsin (*41*), and halorhodopsin in the presence of azide (*42*) possess strongly hydrogen-bonded water molecules (O−D stretch at < 2400 cm^{-1} in D_2O). All of them pump protons. In contrast, strongly hydrogen-bonded water molecules were not observed for halorhodopsin from *Halobacterium salinarum* and *Natronomonas pharaonis* (*22*, *28*), *Neurospora* rhodopsin (*43*), *Anabaena* sensory rhodopsin (*44*), and bovine rhodopsin (*45*). None of them pump protons. In addition, various BR mutants possess strongly hydrogen-bonded water molecules if they pump protons (*24*, *25*). Such comprehensive studies have thus revealed that strongly hydrogen-bonded water molecules are only found in the proteins exhibiting proton-pumping activities. Taken together with the present results for D85S BR mutants, this suggests that strong hydrogen-bonds of water molecules and their transient weakening is needed for the proton-pumping function of rhodopsins.

It was suggested that halide-binding into D85S yields protonation of Asp212 (*10*). This is reasonable, because the distance between Asp212 and halide is short (3.3 Å for Br^-, Figure 1). However, the K minus D85S spectra do not show additional bands in the 1750−1700 cm^{-1} region for any halide-bound forms (Figure 4). If Asp212 is indeed protonated, a new band should appear at this region. At this moment, there are two possibilities. One possibility is that Asp212 is deprotonated even if halide is bound inside, but then the negatively charged Asp212 must be somehow stabilized. The presence of the two positive charges, the Schiff base, and Arg82 may require deprotonation of Asp212 in addition to the bound halide. Another possibility is that Asp212 is protonated, but the C=O group does not undergo a change between the unphotolyzed and K states. Further study on late intermediates will determine the protonation state of Asp212, which is our future focus.

ACKNOWLEDGMENT

We thank Dr. Yuji Furutani for valuable discussions.

REFERENCES

1. Haupts, U., Tittor, J., and Oesterhelt, D. (1999) Closing in on bacteriorhodopsin: Progress in understanding the molecules, *Annu. Rev. Biophys. Biomol. Struct. 28*, 367−399.
2. Lanyi, J. K. (2004) Bacteriorhodopsin, *Annu. Rev. Physiol. 66*, 665−688.
3. Váró, G. (2000) Analogies between halorhodopsin and bacteriorhodopsin, *Biochim. Biophys. Acta 1460*, 220−229.
4. Essen, L.-O. (2002) Halorhodopsin: Light-driven ion pumping made simple? *Curr. Opin. Struct. Biol. 12*, 516−522.
5. Sasaki, J., Brown, L. S., Chon, Y.-S., Kandori, H., Maeda, A., Needleman, R., and Lanyi, J. K. (1995) Conversion of bacteriorhodopsin into a chloride ion pump, *Science 269*, 73−75.
6. Brown, L. S., Needleman, R., and Lanyi, J. K. (1996) Interaction of proton and chloride transfer pathways in recombinant bacteriorhodopsin with chloride transport activity: Implications for the chloride translocation mechanism, *Biochemistry 35*, 16048−16054.
7. Tittor, J., Haupts, U., Haupts, C., Oeaterhelt, D., Becker, A., and Bamberg, E. (1997) Chloride and proton transport in bacteriorhodopsin mutant D85T: Different modes of ion translocation in a retinal protein, *J. Mol. Biol. 271*, 405−416.

8. Luecke, H., Schobert, B., Richter, H.-T., Cartailler, J. P., and Lanyi, J. K. (1999) Structure of bacteriorhodopsin at 1.55 Å resolution, *J. Mol. Biol. 291*, 899−911.
9. Rouhani, S., Cartailler, J.-P., Facciotti, M. T., Walian, P., Needleman, R., Lanyi, J. K., Glaeser, R. M., and Luecke, H. (2001) Crystal structure of the D85S mutant of bacteriorhodopsin: Model of an O-like photocycle intermediate, *J. Mol. Biol. 313*, 615−628.
10. Facciotti, M. T., Cheung, V. S., Lunde, C. S., Rouhani, S., Baliga, N. S., and Glaeser, R. M. (2004) Specificity of anion binding in the substrate pocket of bacteriorhodopsin, *Biochemistry 43*, 4934−4943.
11. Facciotti, M. T., Cheung, V. S., Nguyen, D., Rouhani, S., and Glaeser, R. M. (2003) Crystal structure of the bromide-bound D85S mutant of bacteriorhodopsin: Principles of ion pumping, *Biophys. J. 85*, 451−458.
12. Kolbe, M., Besir, H., Essen, L.-O., and Oesterhelt, D. (2000) Structure of the light-driven chloride pump halorhodopsin at 1.8 Å resolution, *Science 288*, 1390−1396.
13. Aton, B., Doukas, A. G., Callender, R. H., Becher, B., and Ebrey, T. G. (1977) Resonance Raman studies of the purple membrane, *Biochemistry 16*, 2995−2999.
14. Baasov, T., Friedman, N., and Sheves, M. (1987) Factors affecting the C═N stretching in protonated retinal Schiff base: A model study for bacteriorhodopsin and visual pigments, *Biochemistry 26*, 3210−3217.
15. Smith, S. O., Marvin, M. J., Bogomolni, R. A., and Mathies, R. A. (1984) Structure of the retinal chromophore in the hR578 form of the halorhodopsin, *J. Biol. Chem. 259*, 12326−12329.
16. Fodor, S. P. A., Bogomolni, R. A., and Mathies, R. A. (1987) Structure of the retinal chromophore in the hRL intermedeiate of halorhodopsin from resonance spectroscopy, *Biochemistry 26*, 6775−6778.
17. Gerscher, S., Mylrajan, M., Hildebrandt, P., Baron, M.-H., Müller, R., and Engelhard, M. (1997) Chromophore-anion interactions in halorhodopsin form *Natronobacterium pharaonis* probed by time-resolved resonance Raman spectroscopy, *Biochemistry 36*, 11012−11020.
18. Walter, T. J., and Braiman, M. S. (1994) Anion-protein interactions during halorhodopsin pumping: Halide binding at the protonated Schiff base, *Biochemistry 33*, 1724−1733.
19. Lussier, L. S., Sandorfy, C., Le-Thanh, H., and Vocelle, D. (1987) Effect of acids on the infrared spectra of the Schiff base of *trans*-retinal, *J. Phys. Chem. 91*, 2282−2287.
20. Kandori, H., Kinoshita, N., Shichida, Y., and Maeda, A. (1998) Protein structural changes in bacteriorhodopsin upon photoisomerization as revealed by polarized FTIR spectroscopy, *J. Phys. Chem. B 102*, 7899−7905.
21. Kandori, H., Belenky, M., and Herzfeld, J. (2002) Vibrational frequency and dipolar orientation of the protonated Schiff base in bacteriorhodopsin before and after photoisomerization, *Biochemistry 41*, 6026−6031.
22. Shibata, M., Muneda, M., Sasaki, T., Shimono, K., Kamo, N., Demura, M., and Kandori, H. (2005) Hydrogen-bonding alterations of the protonated Schiff base and water molecule in the chloride pump of *Natronobacterium pharaonis*, *Biochemistry 44*, 12279−12286.
23. Kandori, H., and Shichida, Y. (2000) Direct observation of the bridged water stretching vibrations inside a protein, *J. Am. Chem. Soc. 122*, 11745−11746.
24. Shibata, M., Tanimoto, T., and Kandori, H. (2003) Water molecules in the Schiff base region of bacteriorhodopsin, *J. Am. Chem. Soc. 125*, 13312−13313.
25. Shibata, M., and Kandori, H. (2005) FTIR studies of internal water molecules in the Schiff base region of bacteriorhodopsin, *Biochemistry 44*, 7406−7413.
26. Tanimoto, T., Furutani, Y., and Kandori, H. (2003) Structural changes of water in the Schiff base region of bacteriorhodopsin: Proposal of a hydration switch model, *Biochemistry 42*, 2300−2306.
27. Furutani, Y., Shibata, M., and Kandori, H. (2005) Strongly hydrogen-bonded water molecules in the Schiff base region of rhodopsins, *Photochem. Photobiol. Sci. 4*, 661−666.
28. Shibata, M., Muneda, N., Ihara, K., Sasaki, T., Demura, M., and Kandori, H. (2004) Internal water molecules of light-driven chloride pump proteins, *Chem. Phys. Lett. 392*, 330−333.
29. Peck, R. F., DasSarma, S., and Krebs, M. P. (2000) Homologous gene knockout in the archaeon *Halobacterium salinarum* with ura3 as a counterselectable marker, *Mol. Microbiol. 35*, 667−676.
30. Cline, S. W., and Doolittle, W. F. (1987) Efficient transfection of the archaebacterium *Halobacterium* halobium, *J. Bacteriol 169*, 1341−1344.
31. Hu, J. G., Sun, B. Q., Bizounok, M., Hatcher, M. E., Lansing, J. C., Raap, J., Verdegem, P. J. E., Lugtenburg, J., Griffin, R. G., and Herzfeld, J. (1998) Early and late M intermediates in the bacteriorhodopsin photocycle: A solid-state NMR study, *Biochemistry 37*, 8088−8096.
32. Oesterhelt, D., and Stoeckenius, W. (1973) Isolation of the cell membrane of *Halobacterium halobium* and its fractionation into red and purple membrane, *Methods Enzymol. 31*, 667−678.
33. Siebert, F., and Mäntele, W. (1983) Investigation of the primary photochemistry of bacteriorhodopsin by low-temperature Fourier transform infrared spectroscopy, *Eur. J. Biochem. 130*, 565−573.
34. Yamazaki, Y., Tuzi, S., Saitô, H., Kandori, H., Needleman, R., Lanyi, J. K., and Maeda, A. (1996) Hydrogen bonds of water and C═O groups coordinate long-range structural changes in the L photointermediate of bacteriorhodopsin, *Biochemistry 35*, 4063−4068.
35. Braiman, M. S., Mogi, T., Marti, T., Stern, L. J., Khorana, H. G., and Rothschild, K. J. (1988) Vibrational spectroscopy of bacteriorhodopsin mutants: Light-driven proton transport involves protonation changes of aspartic acid residues 85, 96, and 212, *Biochemistry 27*, 8516−8520.
36. Shimono, K., Furutani, Y., Kamo, N., and Kandori, H. (2003) Vibrational modes of the protonated Schiff base in *pharaonis* phoborhodopsin, *Biochemistry 42*, 7801−7806.
37. Eisenberg, D., and Kauzmann, W. (1969) *The Structure and Properties of Water*, Oxford University Press, London.
38. Benedict, W. S., Gailar, N., and Plyler, E. K. (1956) Rotation-vibrarion spectra of deuterated water vapor, *J. Chem. Phys. 24*, 1139−1165.
39. Kandori, H., Shimono, K., Sudo, Y., Iwamoto, M., Shichida, Y., and Kamo, N. (2001) Structural change of *pharaonis* phoborhodopsin upon photoisomerization of the retinal chromophore: Infrared spectral comparison with bacteriorhodopsin, *Biochemistry 40*, 9238−9246.
40. Sumii, M., Furutani, Y., Waschuk, S. A., Brown, L. S., and Kandori, H. (2005) Strongly hydrogen-bonded water molecule present near the retinal chromophore of *Leptosphaeria* rhodopsin, bacteriorhodopsin-like proton pump from a eukaryote, *Biochemistry 44*, 15159−15166.
41. Furutani, Y., Ikeda, D., Shibata, M., and Kandori, H. (2006) Strongly hydrogen-bonded water molecule is observed only in the alkaline form of proteorhodopsin, *Chem. Phys. 324*, 705−708.
42. Muneda, N., Shibata, M., Demura, M., and Kandori, H. (2006) Internal water molecules of the proton-pumping halorhodopsin in the presence of azide, *J. Am. Chem. Soc. 128*, 6294−6295.
43. Furutani, Y., Bezerra, A. G., Jr., Waschuk, S., Sumii, M., Brown, L. S., and Kandori, H. (2004) FTIR spectroscopy of the K photointermediate of *Neurospore* rhodopsin: Structural changes of the retinal, protein, and water molecules after photoisomerization, *Biochemistry 43*, 9636−9646.
44. Furutani, Y., Kawanabe, A., Jung, K.-H., and Kandori, H. (2005) FTIR spectroscopy of the all-trans form of *Anabaena* sensory rhodopsin at 77 K: Hydrogen bond of a water between the Schiff base and Asp75, *Biochemistry 44*, 12287−12296.
45. Furutani, Y., Shichida, Y., and Kandori, H. (2003) Structural changes of water molecules during the photoactivation processes in bovine rhodopsin, *Biochemistry 42*, 9619−9625.
46. Kandori, H., Yamazaki, Y., Shichida, Y., Raap, J., Lugtenburg, J., Belenky, M., and Herzfeld, J. (2001) Tight Asp-85-Thr-89 association during the pump switch of bacteriorhodopsin, *Proc. Natl. Acad. Sci. U.S.A. 98*, 1571−1576.
47. Tanimoto, T., Shibata, M., Belenky, M., Herzfeld, J., and Kandori, H. (2004) Altered hydrogen bonding of Arg82 during the proton pump cycle of bacteriorhodopsin: A low-temperature polarized FTIR spectroscopic study, *Biochemistry 43*, 9439−9447.

BI060555S